Article

Enormously Low Frictional Surface on Tough Hydrogels Simply Created by Laser-Cutting Process

Kazunari Yoshida [1,*] **, Hikaru Yahagi** [1] **, Masato Wada** [2] **, Toshiki Kameyama** [3] **, Masaru Kawakami** [1] **, Hidemitsu Furukawa** [1] **and Koshi Adachi** [4]

[1] Department of Mechanical Systems Engineering, Graduate School of Science and Engineering, Yamagata University, Yamagata 992-8510, Japan; light19940622@gmail.com (H.Y.); kmasaru@yz.yamagata-u.ac.jp (M.K.); furukawa@yz.yamagata-u.ac.jp (H.F.)

[2] Department of Creative Engineering, National Institute of Technology, Tsuruoka College, Yamagata 997-8511, Japan; wada@tsuruoka-nct.ac.jp

[3] Department of Environment and System Sciences, Graduate School of Environment and Information Sciences, Yokohama National University, Yokohama 240-8501, Japan; t.k.isi.ina.7041@gmail.com

[4] School of Mechanical Engineering, Tohoku University, Sendai 980-8579, Japan; koshi@tribo.mech.tohoku.ac.jp

* Correspondence: k-yoshida@yz.yamagata-u.ac.jp; Tel.: +81-238-26-3218

check for updates

Abstract: We measured the friction forces and calculated the friction coefficients of non-processed and laser-processed surfaces of a double network hydrogel (DN gel), which is one of the more famous high-strength gels. The results indicate that laser processing has the ability to reduce the friction coefficients of the gel surfaces. The observation of gel surfaces suggests that the cause of friction reduction is a change in the roughness of the gel surfaces due to laser processing. This finding is expected to lead us to further understanding of the physicochemical properties of hydrogels.

Keywords: friction; hydrogel; lubrication

1. Introduction

Friction and lubrication have been studied for several hundred years. Recently, the friction properties of soft materials, such as polymers and hydrogels, have received attention in regard to their physics and/or physical chemistry. For instance, the friction properties of polymer surfaces have been studied using simulation and experimental methods [1,2]. The results of such fundamental studies are becoming the bases of applications of various fields such as medicine, since it has been shown that such soft materials can be utilized as biomimic materials [3,4].

It is commonly known that hydrogel is one of the beneficial soft materials. To date, the fundamental research studies of functional gels have been reported, e.g., the volume phase transition of gel [5–10], shape memory gel [11], and self-oscillating gel [12,13]. Furthermore, the friction of the hydrogel surface has been studied since the 1990s [14–19], and it has been revealed that hydrogel has a low friction and unique properties in addition to being a bio-inspired film [20,21]. However, such properties have received attention; the friction properties of hydrogels are dependent on their surface conditions, and the controlling of the gel surface is conventionally quite difficult. Hence, novel control methods of surface conditions are required for the further understanding of lubrication.

Double network hydrogel (DN gel) is one of the famous high strength gels [22], and is expected to be applied in various fields. DN gel consists of two types of polymer networks. The first network is rigid and brittle, while the second one is soft and high ductile. The origin of DN gel strength lies on such interpenetrating structures. To make use of such high strength, several groups have

developed the derived types of DN gels such as thermoresponsive and pH-responsive DN gels [23] and three-dimensional (3D) printable DN gels [24]. Furthermore, because the DN gel is also expected to be applied to artificial cartilage in the joints of human legs and/or arms, the low-friction processing of DN gel is quite important.

Previously, the friction properties of DN gel have been studied using a ball-on-plate type apparatus [25,26]. We also developed the friction control technique of hydrogel surfaces [27]. It was revealed that the water molecules inside the hydrogel are moved to interface between the hydrogel and electrode, which then forms the lubricant film owing to the applied electric field, and reduces the friction force. Such a friction control technique is expected to be applied to developing the epoch-making soft-type robots. Conventional-type robots are commonly composed of metals and/or hard plastics. In such cases, robots have a high possibility of causing harm to humans and/or other animals. On the other hand, robots made with soft materials such as hydrogels have a low possibility of causing harm to us. The friction control techniques are required to reduce the dynamical friction of the joint parts of hydrogel robots.

Conventionally, a utility knife and a sawtooth are, for instance, used for the cutting processing. However, it is difficult to cut soft materials, such as hydrogels, using the utility knife and the sawtooth. On the other hand, a laser light has the ability to cut soft materials. Furthermore, a laser light has high directivity and convergence; hence, we are able to easily utilize the laser processing method for micromachining. For instance, an ultrafast laser processing is widely utilized [28].

In this communication, we show a novel method for the low-friction processing of DN gel using a laser, which increases the roughness of the gel surface. We achieved the several micron and several hundred roughness of the gel surfaces using laser processing. The results of friction measurements and microscopic observations suggest that the increase in the roughness of the hydrogel surface reduces the apparent contact area and induces the reduction of the friction coefficient (friction force). It is possible to apply this processing technique to construct artificial living tissues made with various soft materials. It is expected that hydrogels are an appropriate artificial extracellular matrix (ECM) [4]. In addition, many kinds of biological tissues are low-friction [29]; hence, this technique is beneficial for constructing the artificial living tissues. Furthermore, the properties of artificial cell membranes have been widely studied to clarify the physicochemical mechanisms governing the behaviors of living cell membranes [30–37], and 3D hydrogel printing techniques [24,38] have been developed in the related fields. By utilizing low-friction processing and such previously obtained knowledges and techniques, artificial living tissues composed of cell models and polymer gel ECMs can be developed.

2. Experimental Section

2.1. Preparation of DN gel

First, we prepared an aqueous solution including a 2-acrylamideo-2-methylpropanesulfonic acid (AMPS, Sigma-Aldrich Co. LLC. St. Louis, MO, USA) monomer, a *N,N′*-methylenebisacrylamide (MBAA, Wako Pure Chemical Industries, Ltd. Osaka, Japan) crosslinker, and a 2-Oxoglutaric Acid (α-keto, Wako Pure Chemical Industries, Ltd. Osaka, Japan) photo-initiator by stirring with N_2 gas bubbling to remove the O_2 gas included in the solution for 10 min to 15 min. The concentration of the AMPS monomer was 1 M. The concentrations of the crosslinker and photo-initiator were 4 mol % and 0.1 mol % in the solute, respectively. Furthermore, the solution was sandwiched by two glass plates with 2-mm spacing, and was then exposed by ultraviolet (UV) light (λ_{max} = 365 nm, *ca.* 0.1 mW/cm^2) at 30 °C for more than 18 h to make the first polymer network.

The first gel was swollen in a second pregel solution for 48 h. The second pregel solution contained 2 M of *N,N*-Dimethylacrylamide (DMAAm, Tokyo Chemical Industry Co., Ltd. Tokyo, Japan) monomer, 0.01 mol % (molar percentage in the solute) of MBAA, and 0.05 mol % of α-keto. The second pregel solution was also prepared by stirring and N_2 gas bubbling with the same procedure as in the case of the first pregel solution. The first gel was cut to remove part of the polymerization residue. The first gel that was swollen

in the second pregel solution was sandwiched by two glass plates and exposed by UV light with the same condition as described above. The DN gel was then swollen in a large amount of pure water for three days. The final thickness of the DN gel was 5 mm.

2.2. Laser Processing

We used the laser cutter VLS 4.60 (Yokohama Systems Co. Ltd. Yokohama, Japan) for low-friction processing. The laser power is 60 W per spot area (0.127 mm in diameter). The laser density during processing is 200 pulses per inch (PPI) with a vector mode. The laser light is in focus at the upper surface of the gel samples. We cut the prepared DN gel plate into 5 mm × 65 mm size.

We observed the gel surfaces by using an optical microscope BX50 (Olympus Corp. Tokyo, Japan) equipped with a digital camera DP72 (Olympus Corp. Tokyo, Japan) to elucidate the difference between the non-processed and laser-processed gel surfaces. Figure 1 shows the microscopic images of non-processed and laser-processed gel surfaces. The roughness of the gel surface was larger for the laser-processed gel surface than for the non-processed one. In Figure 1a, there is a thin line pattern. This pattern naturally appeared during gel preparation. The diameters of such lines were several microns. On the other hand, larger patterned roughness was observed in Figure 1b, and the wavelength of surface waviness was approximately several tens microns and several hundred microns. This indicates that the melting and/or vaporization of the gel sample was induced by laser light [39], and the roughness of the gel surface was increased due to such melting and/or vaporization. In the case of a higher intensity of laser and/or slower scan speed than the conditions of this study, it is speculated that the surface roughness would become larger than several tens microns due to the increasing damage of the gel surface.
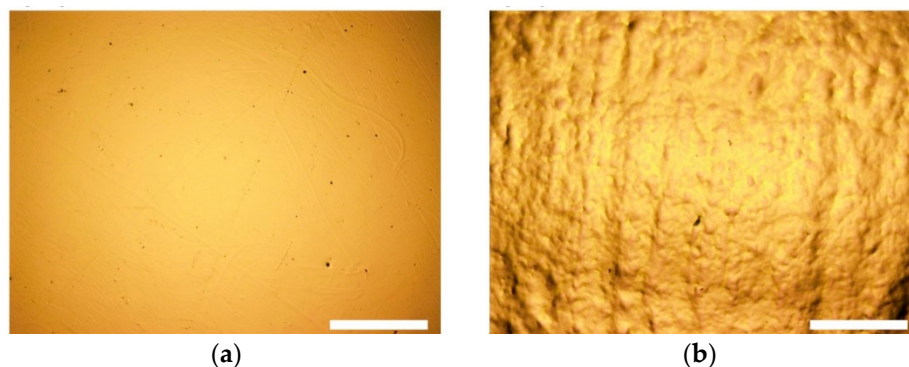

(**a**)   (**b**)

Figure 1. Typical microscopic images of (**a**) non-processed (control) and (**b**) laser-processed gel surfaces. The roughness of the gel surface is larger at the laser-processed gel surface than at the non-processed one. Scale bars represent 500 μm.

2.3. Friction Measurements

The surface frictions of the DN gels were measured using a ball-on-plate type apparatus μV1000 (Trinity-Lab. Inc. Tokyo, Japan). The glass ball used in this study (BK7, ϕ6 mm) was washed by Neo-ethanol IPM (Daishin Chemistry Co. Ltd. Tokyo, Japan) before the experiments. The DN gel samples were attached on an acrylic plate using an Aron Alpha for institutional use (Toagosei Co., Ltd. Tokyo, Japan). The normal load was 300 g of weight during the experiments. We measured the friction properties at one series with a seven-step sliding-velocity change. The sliding velocities were 0.1 mm/s, 0.5 mm/s, 1.0 mm/s, 5.0 mm/s, 10.0 mm/s, 50.0 mm/s, and 100.0 mm/s, and the sliding lengths were 1 mm, 2 mm, 2 mm, 5 mm, 5 mm, 10 mm, and 25 mm at each velocity, respectively. The five-times series were performed on the same place of each sample, and we calculated the averaged value using last three-times data. Such five-series experiments were performed three times with different areas of the samples cut from the same large gel plates. We compared between the friction properties of the gel

surfaces that came into contact with the glass plate during polymerization (control, non-processed surface) and the laser-processed gel surface. We defined the measured values of the friction force as the time-averaged values of the stable regions. Figure 2 shows the schematic illustration of the experimental set-up of the friction measurements.
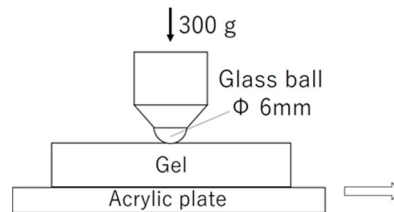

Figure 2. Schematic illustration of experimental set-up of friction measurements. The lower plate was moved during the measurements.

3. Results and Discussion

We measured the friction force and estimated the friction coefficient (μ) of the DN gel surfaces without and with laser processing. The friction coefficient is defined as follows:

$$\mu = F/W, \tag{1}$$

where F is the friction force and W is the normal load. In this study, the normal load was constantly 300 g of weight. During friction measurement, the DN gel samples were placed and attached onto the acrylic plate stage, and the gel surfaces were in contact with the measurement ball, as described above.

Figure 3 shows the friction coefficient derived from the friction force and normal load as a function of sliding velocity (mean $\pm$ standard deviation). The friction properties were independent of the sliding direction. In terms of the result of the non-processed gel surface, the behavior shown in Figure 3 corresponds to the range from boundary lubrication to mixed lubrication, as described below. The range of the friction coefficients was approximately 0.01–0.1. The friction coefficient increased with the increasing sliding velocity in the range of 0.1–0.5 mm/s. In contrast, the friction coefficient decreased with the increasing sliding velocity in the range of 0.5–10 mm/s. In addition, the friction coefficient was almost constant in the range of 10–100 mm/s. Such behavior was observed in both cases of non-processed and laser-processed gel surfaces, which is in good agreement with the previous work [25]. The interaction between the polymers in the hydrogels and the glass measurement ball is important in the low-velocity range [14,15]. In case of an attractive substrate, the friction force as a function of the sliding velocity has a peak due to the relationship between the stretching of the polymer chains with adsorption to the glass ball and the sliding velocity. This behavior was discussed by using a mathematical model in the previous work [15]. Hence, it is speculated that the cause of the peak appearance at 0.5 mm/s that is shown in Figure 3 is the same as the cause shown in the previous work. In the high-velocity range, the sliding velocity becomes faster than the adsorption rate of polymers to the glass ball. Hence, hydrodynamic lubrication becomes dominant compared to boundary lubrication. For the results of Figure 3, it is considered that the range of 0.1–0.5 mm/s corresponds to boundary lubrication, while the range of 0.5–100 mm/s corresponds to mixed lubrication. It is speculated that the friction force (friction coefficient) is increased with the increase in the sliding velocity due to hydrodynamic lubrication in the range of 100 mm/s and above. Furthermore, the friction coefficient is larger at the non-processed gel surface than at the laser-processed one in all of the velocity regions, and such behavior is remarkable in the range of boundary lubrication (0.1–0.5 mm/s). The results show that this laser processing has the ability to reduce the friction coefficient of the hydrogel surfaces.
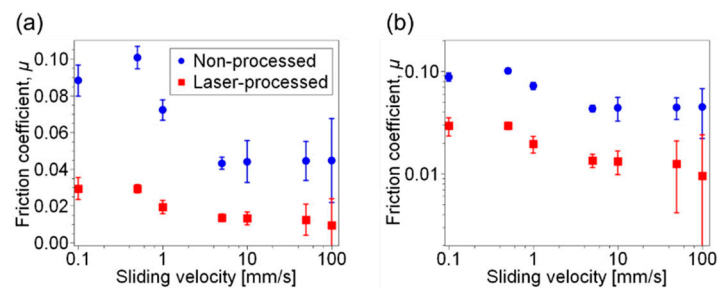
Figure 3. The friction coefficient as a function of the sliding velocity in the cases of non-processed and laser-processed gel surfaces. The vertical axes are (**a**) linear and (**b**) logarithmic scales (mean ± standard deviation).

Figure 4 shows a schematic illustration of the difference between before and after laser processing in the case of the glass ball and hydrogel interface. Large roughness was observed in the caser of the laser-processed gel surface as shown above, and this roughness was approximately several tens microns (see Figure 1b). It is considered that the melting and/or vaporization of the gel sample was induced by laser light [39], and the large roughness of the gel surface was created through such melting and/or vaporization. The results of microscopic observation and friction measurements suggest that an increase in the surface roughness has the ability to reduce the friction coefficient. It is considered that the decrease in the apparent contact area reduces the interaction between the polymers in the gel and the measurement of the glass ball. This is consistent with the equation $F \propto AP^{\alpha}$, where A is the apparent contact area, $P = W/A$ is the averaged pressure, and α $(0 \leq \alpha \leq 1)$ is derived from experiments [16], which indicates that the friction coefficient depends on the apparent contact area.
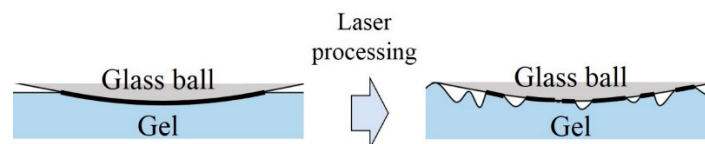

Figure 4. Schematic illustration of the difference between before and after laser processing in the case of the glass ball and hydrogel interface. Bold curves represent the true contacting interface.

It is considered that further experiments are required to elucidate a detailed mechanism of friction reduction by laser processing. For instance, an in situ microscopic observation of the contact interface during sliding is required to clarify the dynamic behaviors of the surface conditions. Furthermore, resonance shear measurement (RSM) is beneficial to elucidate the viscoelastic properties of hydrogel [19]. Utilizing this method, the gel surface was observed during friction measurements, and we were able to obtain the value of the contact area.

To clarify the detailed structure of laser-processed gel surfaces, the observation of gel samples using an atomic force microscope (AFM) [40] and/or cryogenic scanning electron microscope (Cryo-SEM) [41] is required. We observed the gel surfaces using an optical microscopy in this study; however, the observation results are not enough for clarifying the fragility analysis of the gel surfaces. We are able to obtain the information at a smaller scale using an AFM compared with using an optical microscope.

4. Conclusions

In conclusion, we showed the low-friction processing technique of the hydrogel surface. We demonstrated that the laser processing has an ability to reduce the friction of the hydrogel. The results of the microscopic observations suggest that the cause of friction reduction is a decrease in

the apparent contact area between the hydrogel surface and the glass ball. This technique may lead us to the next step in the fields of physics, physical chemistry, soft robotics, and medical applications.

5. Patents

The patent of this low-friction processing technique is pending: H.F.; M.K.; M.W.; T.K.; K.A. Multi-Joined Manipulator. Japan patent application 2017-022098.

References

1. Otsuki, M.; Matsukawa, H. Systematic Breakdown of Amontons' Law of Friction for an Elastic Object Locally obeying Amontons' Law. *Sci. Rep.* **2013**, *3*, 1586. [CrossRef] [PubMed]
2. Katano, Y.; Nakano, K.; Otsuki, M.; Matsukawa, H. Novel Friction Law for the Static Friction Force based on Local Precursor Slipping. *Sci. Rep.* **2014**, *4*, 6324. [CrossRef] [PubMed]
3. Miyata, T.; Asami, N.; Uragami, T. A Reversibly Antigen-Responsive Hydrogel. *Nature* **1999**, *399*, 766–769. [CrossRef] [PubMed]
4. Green, J.J.; Elisseeff, J.H. Mimicking Biological Functionality with Polymers for Biomedical Applications. *Nature* **2016**, *540*, 386–394. [CrossRef] [PubMed]
5. Tanaka, T. Collapse of Gels and the Critical Endpoint. *Phys. Rev. Lett.* **1978**, *40*, 820. [CrossRef]
6. Tanaka, T.; Fillmore, D.; Sun, S.-T.; Nishio, I.; Swislow, G.; Shah, A. Phase Transitions in Ionic Gels. *Phys. Rev. Lett.* **1980**, *45*, 1636. [CrossRef]
7. Tanaka, T.; Nishio, I.; Sun, S.-T.; Ueno-Nishio, S. Collapse of Gels in an Electric Field. *Science* **1982**, *218*, 467–469. [CrossRef] [PubMed]
8. Hirokawa, Y.; Tanaka, T. Volume phase transition in a nonionic gel. *J. Chem. Phys.* **1984**, *81*, 6379. [CrossRef]
9. Arai, K.D.; Saito, A.; Ito, K.; Uematsu, Y.; Ueno, T.; Fujii, Y.; Nishio, I. Isobars, the Coexistence Curve, and the Critical Exponent *β* of *N*-Isopropylacrylamide Gels Obtained Using A Simple Experimental Method. *Phys. Rev. E* **2013**, *87*, 022603. [CrossRef] [PubMed]
10. Saito, A.; Kimura, J.; Fujii, Y.; Nishio, I. Volume Phase Transition of *N*-Isopropylacrylamide Gels Crosslinked by a Crosslinker with Six Hands. *Phys. Rev. E* **2013**, *88*, 062601. [CrossRef] [PubMed]
11. Osada, Y.; Matsuda, A. Shape Memory in Hydrogels. *Nature* **1995**, *376*, 219. [CrossRef] [PubMed]
12. Yoshida, R.; Takahashi, T.; Yamaguchi, T.; Ichijo, H. Self-Oscillating Gel. *J. Am. Chem. Soc.* **1996**, *118*, 5134–5135. [CrossRef]
13. Yoshida, R.; Takahashi, T.; Yamaguchi, T.; Ichijo, H. Self-Oscillating Gels. *Adv. Mater.* **1997**, *9*, 175–178. [CrossRef]
14. Gong, J.P.; Higa, M.; Iwasaki, Y.; Katsuyama, Y.; Osada, Y. Friction of Gels. *J. Phys. Chem. B* **1997**, *101*, 5487–5489. [CrossRef]
15. Gong, J.P.; Osada, Y. Gel Friction: A Model Based on Surface Repulsion and Adsorption. *J. Chem. Phys.* **1998**, *109*, 8062. [CrossRef]
16. Gong, J.P.; Iwasaki, Y.; Osada, Y.; Kurihara, K.; Hamai, Y. Friction of Gels. 3. Friction on Solid Surfaces. *J. Phys. Chem. B* **1999**, *103*, 6001–6006. [CrossRef]

17. Gong, J.P. Friction and Lubrication of Hydrogels—Its Richness and Complexity. *Soft Matter* **2006**, *2*, 544–552. [CrossRef]
18. Kosukegawa, H.; Fridrici, V.; Kapsa, P.; Sutou, Y.; Adachi, K.; Ohta, M. Friction Properties of Medical Metallic Alloys on Soft Tissue-Mimicking Poly(Vinyl Alcohol) Hydrogel Biomodel. *Tribol. Lett.* **2013**, *51*, 311–321. [CrossRef]
19. Ren, H.-Y.; Mizukami, M.; Tanabe, T.; Furukawa, H.; Kurihara, K. Friction of Polymer Hydrogels Studied by Resonance Shear Measurements. *Soft Matter* **2015**, *11*, 6192–6200. [CrossRef] [PubMed]
20. Kanda, K.; Sato, H.; Miyakoshi, T.; Kitano, T.; Kanebako, H.; Aadachi, K. Friction Control of Mechanical Seals in a Ventricular Assist Device. *Biosurf. Biotribol.* **2015**, *1*, 135–143. [CrossRef]
21. Kanda, K.; Adachi, K. Shear Strength of Protein Film Formed by Friction of SiC/SiC Sliding Pair in Plasma Environment. *Biotribology* **2017**, *10*, 26–34. [CrossRef]
22. Gong, J.P.; Katsuyama, Y.; Kurokawa, T.; Osada, Y. Double-Network Hydrogels with Extremely High Mechanical Strength. *Adv. Mater.* **2003**, *15*, 1155–1158. [CrossRef]
23. Li, Z.; Shen, J.; Ma, H.; Lu, X.; Shi, M.; Li, N.; Ye, M. Preparation and Characterization of pH- and Temperature-Responsive Nanocomposite Double Network Hydrogels. *Mater. Sci. Eng. C* **2013**, *33*, 1951–1957. [CrossRef] [PubMed]
24. Muroi, H.; Hidema, R.; Gong, J.; Furukawa, H. Development of Optical 3D Gel Printer for Fabricating Free-Form Soft & Wet Industrial Materials and Evaluation of Printed Double-Network Gels. *J. Solid Mech. Mater. Eng.* **2013**, *7*, 163–168.
25. Wada, M.; Hidema, R.; Chiba, T.; Yamada, K.; Yamada, N.; Gong, J.; Furukawa, H. Surface and Bulk Mechanical Properties of Soft and Wet Materials. *J. Solid Mech. Mater. Eng.* **2013**, *7*, 228–234. [CrossRef]
26. Wada, M.; Kameyama, T.; Arai, M.; Yamada, K.; Makino, M.; Kawakami, M.; Furukawa, H. Friction Measurement of Functional Gel Mechanical Materials. *Microsyst. Technol.* **2016**, *22*, 77–81. [CrossRef]
27. Wada, M.; Yamada, K.; Kameyama, T.; Yamada, N.; Yoshida, K.; Saito, A.; Makino, M.; Khosla, A.; Kawakami, M.; Furukawa, H. Electric Control of Friction on Surface of High-Strength Hydrogels. *Microsyst. Technol.* **2018**, *24*, 639–646. [CrossRef]
28. Malinauskas, M.; Žukauskas, A.; Hasegawa, S.; Hayasaki, Y.; Mizeikis, V.; Buividas, R.; Juodkazis, S. Ultrafast Laser Processing of Materials: from Science to Industry. *Light: Sci. Appl.* **2016**, *5*, e16133. [CrossRef]
29. Jin, Z.; Dowson, D. Bio-friction. *Friction* **2013**, *1*, 100–113. [CrossRef]
30. Baumgart, T.; Hess, S.T.; Webb, W.W. Imaging Coexisting Fluid Domains in Biomembrane Models Coupling Curvature and Line Tension. *Nature* **2003**, *425*, 821–824. [CrossRef] [PubMed]
31. Hamada, T.; Sugimoto, R.; Vestergaard, M.C.; Nagasaki, T.; Takagi, M. Membrane Disc and Sphere: Controllable Mesoscopic Structures for The Capture and Release of a Targeted Object. *J. Am. Chem. Soc.* **2010**, *132*, 10528–10532. [CrossRef] [PubMed]
32. Hamada, T.; Morita, M.; Miyakawa, M.; Sugimoto, R.; Hatanaka, A.; Vestergaard, M.C.; Takagi, M. Size-Dependent Partitioning of Nano/Micro-Particles Mediated by Membrane Lateral Heterogeneity. *J. Am. Chem. Soc.* **2012**, *134*, 13990–13996. [CrossRef] [PubMed]
33. Morita, M.; Hamada, T.; Vestergaard, M.C.; Takagi, M. Endo- and Exocytic Budding Transformation of Slow-Diffusing Membrane Domains Induced by Alzheimer's Amyloid Beta. *Phys. Chem. Chem. Phys.* **2014**, *16*, 8773–8777. [CrossRef] [PubMed]
34. Yoshida, K.; Fujii, Y.; Nishio, I. Deformation of Lipid Membranes Containing Photoresponsive Molecules in Response to Ultraviolet Light. *J. Phys. Chem. B* **2014**, *118*, 4115–4121. [CrossRef] [PubMed]
35. Yoshida, K.; Horii, K.; Fujii, Y.; Nishio, I. Real-Time Observation of Liposome Bursting Induced by Acetonitrile. *ChemPhysChem* **2014**, *15*, 2609–2912. [CrossRef] [PubMed]
36. Yoshida, K.; Takashima, A.; Nishio, I. Effect of Dibucaine Hydrochloride on Raft-Like Lipid Domains in Model Membrane Systems. *MedChemComm* **2015**, *6*, 1444–1451. [CrossRef]
37. Yoshida, K.; Mitsumori, R.; Horii, K.; Takashima, A.; Nishio, I. Acetonitrile-Induced Destabilization in Liposomes. *Colloids Interfaces* **2018**, *2*, 6. [CrossRef]
38. Ota, T.; Yoshida, K.; Tase, T.; Sato, K.; Tanaka, M.; Saito, A.; Takamatsu, K.; Kawakami, M.; Furukawa, H. Influence of 3D-Printing Conditions on Physical Properties of Hydrogel Objects. *Mech. Eng. J.* **2018**, *5*, 17-00538. [CrossRef]

39.   Ion, J. *Laser Processing of Engineering Materials: Principles, Procedure and Industrial Application*; Butterworth-Heinemann: Oxford, UK, 2005.

40.   Pirani, F.; Sharma, N.; Moreno-Cencerrado, A.; Fossati, S.; Petri, C.; Descrovi, E.; Toca-Herrera, J.L.; Jonas, U.; Dostalek, J. Optical Waveguide-Enhanced Diffraction for Observation of Responsive Hydrogel Nanostructures. *Macromol. Chem. Phys.* **2017**, *218*, 1600400. [CrossRef]

41.   Nykanen, A.; Nuopponen, M.; Hiekkataipale, P.; Hirvonen, S.-P.; Soininen, A.; Tenhu, H.; Ikkala, O.; Mezzenga, R.; Ruokolainen, J. Direct Imaging of Nanoscopic Plastic Deformation below Bulk T_g and Chain Stretching in Temperature-Responsive Block Copolymer Hydrogels by Cryo-TEM. *Macromolecules* **2008**, *41*, 3243–3249. [CrossRef]